

R. Cesario, L. Amicucci, A. Fonseca, I. Chapman, F. Jenko, M. Marinucci,  
S. Saarelma, P. Smeulders, D. Told, R. Zagorski, J. Baranov, M. Beurskens,  
R. De Angelis, D. Mc Donald, C. Challis, A. Galli, J. Mailloux, V. Pericoli,  
and JET EFDA contributors

# Low-Recycling Conditions and Improved Core Confinement in Steady-State Operation Scenarios in JET (Joint European Torus)

“This document is intended for publication in the open literature. It is made available on the understanding that it may not be further circulated and extracts or references may not be published prior to publication of the original when applicable, or without the consent of the Publications Officer, EFDA, Culham Science Centre, Abingdon, Oxon, OX14 3DB, UK.”

“Enquiries about Copyright and reproduction should be addressed to the Publications Officer, EFDA, Culham Science Centre, Abingdon, Oxon, OX14 3DB, UK.”

The contents of this preprint and all other JET EFDA Preprints and Conference Papers are available to view online free at [www.iop.org/Jet](http://www.iop.org/Jet). This site has full search facilities and e-mail alert options. The diagrams contained within the PDFs on this site are hyperlinked from the year 1996 onwards.

# Low-Recycling Conditions and Improved Core Confinement in Steady-State Operation Scenarios in JET (Joint European Torus)

R. Cesario<sup>1</sup>, L. Amicucci<sup>2</sup>, A. Fonseca<sup>3</sup>, I. Chapman<sup>4</sup>, F. Jenko<sup>5</sup>, M. Marinucci<sup>1</sup>,  
S. Saarelma<sup>4</sup>, P. Smeulders<sup>1</sup>, D. Told<sup>5</sup>, R. Zagorski<sup>6</sup>, J. Baranov<sup>4</sup>, M. Beurskens<sup>4</sup>,  
R. De Angelis<sup>1</sup>, D. Mc Donald<sup>4</sup>, C. Challis<sup>3</sup>, A. Galli<sup>2</sup>, J. Mailloux<sup>3</sup>, V. Pericoli<sup>1</sup>,  
and JET EFDA contributors\*

*JET-EFDA, Culham Science Centre, OX14 3DB, Abingdon, UK*

<sup>1</sup>*Associazione EURATOM/ENEA sulla Fusione, Centro Ricerche Frascati c.p. 65, 00044 Frascati, Italy*

<sup>2</sup>*Università di Roma La Sapienza, Facoltà di Ingegneria, Via Eudossiana, Roma*

<sup>3</sup>*Associação EURATOM/IST Centro de Fusão Nuclear, 1049-001 Lisbon, Portugal*

<sup>4</sup>*EURATOM-CCFE Fusion Association, Culham Science Centre, OX14 3DB, Abingdon, OXON, UK*

<sup>5</sup>*Max Planck IPP Garching Germany*

<sup>6</sup>*EFDA Garching Germany*

\* See annex of F. Romanelli et al, "Overview of JET Results",  
(23rd IAEA Fusion Energy Conference, Daejeon, Republic of Korea (2010)).



## ABSTRACT.

It is described the effect of plasma operations producing low particle recycling from the vessel walls during the L-mode (prelude) phase, on core confinement in the H-mode (main heating) phase. Available data of experiments of JET are considered, aimed at approaching fully non-inductive ITER-relevant conditions. The relatively high electron temperature produced at the edge by the initial  $D\alpha$  level condition, results favouring the build-up of high normalised  $\beta$  ( $\beta_N$ ) regimes, in which the confinement is improved in large plasma volume. Modelling of turbulence of the edge, transport, stability and current profile evolution helps interpreting this complex phenomenology, indicating a link between the values at the edge of electron temperature, bootstrap current density and local magnetic shear and the confinement in the core. Such link would favour these regimes to be self-sustained in the time.

## 1. INTRODUCTION

Full control of plasma current profile represents the next main objective for the progress of the thermonuclear fusion research, based on the tokamak concept [1], towards a steady-state (SS) energy source. For these reasons, in order to improve stability and confinement, it would be necessary to optimise the plasma current profile evolution [2–4]. In this context, utilising the lower hybrid current drive (LHCD) effect [5], significant progresses were produced on JET consisting in long-lasting transport barriers (TBs) with relatively large radial foot (at  $\rho \approx 0.6$ – $0.7$ , where  $r$  is the normalised toroidal flux coordinate). A plasma shape with low triangularity ( $\delta \approx 0.2$ ), plasma current ( $I_p$ ) of 1.5MA, toroidal magnetic field ( $B_T$ ) of 3.45T, safety factor at the edge ( $q_{\text{edge}}$ ) of about 8 were utilised. In these experiments, an H-mode is produced by an externally launched power, provided by neutral beam (NB) and ion cyclotron resonant heating (ICRH) systems, applied after the end of the plasma current ramp-up (prelude phase). The cause of the observed TBs was identified in the low magnetic shear produced by LHCD power externally coupled during the H-mode phase [9,10].

In order to develop SS regimes at high normalised  $\beta$  ( $\beta_N$ ), a plasma shaped with high triangularity ( $\delta \approx 0.4$ ) was utilised in experiments of JET at  $I_p = 1.5\text{MA}$ ,  $B_T = 3.45\text{ T}$ ,  $q_{95} \sim 7$ – $7.5$ , which obtained TBs with larger radial size ( $\delta \approx 0.8$ ) yielding  $H_{89} \approx 2.0$ , and normalized beta  $\beta_N \sim 2$  [12]. More recently, operations in the same configuration of high triangularity plasma ( $\delta \approx 0.4$ ) were performed, but with an ITER-relevant lower  $q_{95}$  ( $\approx 5$ ), obtained with  $I_p = 1.5\text{MA}$ ,  $B_T = 2.3\text{T}$  [8–10], or with a slightly higher toroidal magnetic field ( $B_T = 2.7\text{T}$ ) in order to improve ICRH in the core ( $I_p = 1.8\text{ MA}$  for obtaining the same  $q_{95} \approx 5$ ) [11]. In the extensive experimental campaigns that utilised this plasma configuration, an improved confinement up to  $\beta_N \sim 3$  was obtained. Unfortunately, the LHCD effect was not produced in such plasmas, as the plasma shaped with high triangularity produced high plasma densities even at the edge, having the consequence of preventing the penetration of the coupled radiofrequency power in the core [6]. However, these density profiles represent a feature essential for approaching ITER requirements for SS operations.

We consider here available data of the aforementioned homogeneous group of experiments

of JET [8–11] that have contributed developing ITER-relevant SS regimes at high  $\beta_N$ . During the campaigns, dedicated experiments were performed for assessing the role of two different gas fuelling waveforms in prelude in affecting the level of the particle recycling for the vessel walls, with some possible consequent effects on confinement performance during the H-mode phase. The obtained results have suggested reconsidering previous experiments and their modelling in a new light. Indeed, the  $\beta_N$  performance occurring during the main heating phase appears linked to the recycling level measured before the switch-on of the main heating power.

The present paper focuses on initial operating conditions of plasma edge that result useful for improving confinement. Some complex mechanism, possibly linked to current drive, should be involved. Incidentally, similar edge conditions are also useful for extending to reactor grade high plasma density the occurrence of LHCD, which instead resulted ineffective in standard operations with high plasma densities, including the aforementioned of JET [6]. Experiments on FTU have demonstrated that the LHCD effect is enabled to occur at densities even higher than in ITER, provided that the plasma target of the LH (lower hybrid) power should be prepared with a proper condition that produces a higher temperature at the plasma edge [7]. This condition is similar to that shown here as useful for improving confinement performance. Considering the high efficiency in driving current by LH waves, the problem of how sustain the effect of the bootstrap current fraction in tokamaks would be enormously simplified by the use of the LHCD effect, made possible by operations that also promote confinement improvement.

We show results of modelling that support the hypothesis that the phenomenological link between initial condition of recycling and confinement performance should be the effect of the current drive and magnetic shear on confinement and stability, favoured by a higher temperature occurring at the plasma edge, consequence of the low recycling condition. In a further work, we will show that the condition of low recycling is useful also to promote, in the context of experiments taken into account here, the occurrence of LHCD effect.

The paper is organised as follows: Sec.2 shows the statistics that demonstrates, for given conditions of experiments of JET aimed at developing ITER-relevant SS regimes, the link between the initial condition of recycling and  $\beta_N$  performance during H-mode phase; Sec.3 presents a summary of previous AT experiments that produced  $\beta_N$  performances obtained via optimisation that included a lower recycling before the NB power switch-on time; Sec.4 shows model results linking the particle recycling to kinetic profiles at the plasma edge; in Sec.5 an hypothesis is formulated which interprets the considered phenomenology; Sec.6 is dedicated to comments and conclusions.

## **2. PHENOMENOLOGY OF THE RECYCLING IN L-MODE PHASE AND CONFINEMENT DURING H-MODE PHASE**

The link between the particle recycling from the vessel walls in L-mode phase and confinement in H-mode is shown here as result of a phenomenology occurring in the more recent experiments of JET, recalled in the previous section, aimed at developing ITER-relevant SS scenarios at high  $\beta_N$

[11]. This phenomenology has been obtained by statistics carried out on a wide group of plasma discharges performed with same operating parameters (plasma configuration, toroidal magnetic field, plasma current, density and timing of the main heating power) with the exception, for some of them, of using a different gas fuelling waveform in prelude. In any case the same value of density for the plasma target of the main heating power was however maintained. Since these experiments were aimed at maximising the main heating power for confinement improvement, a wide number of similar plasma discharges was performed, which resulted useful indeed for the statistics in object. These experiments were performed in the last four experimental sessions that concluded the operations of JET in carbon wall.

Although the experiments performed for developing SS scenarios by utilising same parameters of plasma configuration, density,  $q_{95}$ , and timing of the main heating power consisted in a wider group of discharges, we consider here only pulses with matched parameters that presented only some difference in the initial level of recycling due to minor changes of the operating conditions occurring shot-by-shot, or due to a different gas fuelling waveform utilised in prelude that, however, guaranteed obtaining the same reference plasma density when the NB power was switched-on. This choice of considering only plasmas in the same configuration and with matched operating parameters (of plasma current, magnetic field, plasma density,  $q_{95}$ , and timing of the main heating power) was necessary for ascertaining the occurrence of a dependence of the confinement performance in H-mode on the initial level of recycling. We would however extend the analysis, in the next sections, including experiments performed in the same plasma configuration and same density,  $q_{95}$ , and timing of the main heating power, but with some difference in the prelude phase consisting in LH or purely ohmic prelude and with less gas fuelled in prelude producing a lower recycling and also a lower density of the plasma target of the main heating power.

In order to include several cases with not too matched values of main heating power, however lying within a spread of less than 20% (which reflects the attempts for enhancing the coupled power) the  $\beta_N$  has been normalised to the main heating power. Nevertheless, the main conclusion of the statistics can be drawn also without considering this normalisation, as the sub-group of discharges with matched power is sufficiently wide.

The monitored change of recycling was due to: i) the two different gas fuelling waveforms in the L-mode (prelude) phase, which produced, however, the same density of the main heating power plasma target, ii) minor changes of gas fuelling that were automatically imposed by the feedback system for maintaining, shot by shot, the same target density. The operation with less gas fuelling before switching-on the NB power, utilised in the last couple of sessions, is referred to as early gas fuelling overshoot. This technique consists in tuning the gas level with a proper abundance in the early prelude (within the time window  $t = 1.0s - 2.0s$ ), and less gas (about 30%) in the late prelude phase (from  $t > 2.0s$  up to  $t_{NB}$ ), with the constraint of obtaining the same density for the plasma target of the NB power, i.e., at the time  $t_{NB}$  just before the NB switch-on. This technique was aimed at preparing plasma targets of the main heating power with a lower recycling with possible effect

on confinement, as suggested by previous experiments [13–15] and signatures on JET mentioned hereafter in the paper.

In order to assess the evolution of recycling, the available data of all diagnostics monitoring the  $D\alpha$  emission along different lines of sights of main chamber and divertor, have been considered. Namely, the signals from the lines of sight horizontal and vertical of the main vessel, and from the divertor, respectively, in the low and high field sides have been considered [18]. Focussing in the initial condition of recycling, in all discharges, the evolution of the  $D\alpha$  signal in L-mode phase and the  $\beta_N$  during H-mode has been monitored. The conditions of the analysis are displayed in Figure 1, which shows the time evolution of the relevant parameters of a couple of discharges of the considered homogeneous group of experiments.

Figure 1f shows the two different gas waveforms utilised in late prelude. The statistics considers the average of the  $D\alpha$  signal levels kept at the time  $t_{NB}$ . In most discharges, the maximum  $\beta_N$  occurs quite soon after the start of the main heating phase, see Fig.1h. However, since the experiments were aimed at developing scenarios towards the steady-state, we focussed in monitoring the relative maximum  $\beta_N$  occurring later (2.5s – 3.5s) after the time point  $t_{NB}^-$ . Therefore, for discharges that exhibit a sufficiently sustained high  $\beta_N$  phase (more than 1 s), the  $\beta_{N\_max}$  has been considered within the time window  $t = 6.5s - 7.5s$ . This choice enables making more evident a possible link between edge physics in L-mode and the behaviour of the H-mode well after his formation. The data analysis was performed considering the available data of all comparable discharges. The exact power level (within 0.5%) was considered in the relevant time window for measuring the occurring changes of maximum  $\beta_N$  (of the order of several percent).

The statistics for the considered group of discharges is shown in Figure 2. The trend of the maximum  $\beta_N$  (normalised to the main heating power) monitored in the late H-mode phase, is plotted against the average of the  $D\alpha$  signal levels measured at the time point  $t_{NB}$ . The displayed dashed segments link together cases with exactly matched values of main heating power, which however did not change too much in the other cases (in the range of 25MW – 34MW). The most relevant outcome of Fig.2 would consist in the amount of 100% of coincident cases linking a lower initial recycling to a higher max  $\beta_N$ . Therefore, the supposed dependence of variables should be considered, indeed, fully assessed, so that we can conclude that, for the considered conditions of experiment, the lower the initial recycling near the end of the L-mode phase, the higher the  $\beta_N$  in late H-mode phase. In particular, during the experiments, both discharges 77875 and 77895 of Fig.2 obtained the highest  $\beta_N$  ( $\approx 3$ ), but the former had a main heating power (27MW) less than the latter (34MW) and an initial recycling slightly lower (of 5%).

The statistics enables concluding that, in the considered plasma conditions, a marked reduction of the  $D\alpha$  level ( $\sim 30\%$ ) would produce a significant increase of  $\beta_N$  ( $\sim 20\%$ ).

In order to assess the way in which changes of the initial recycling level in L-mode affect confinement performance in H-mode, we have searched for changes of kinetic profiles occurring in prelude, in particular, at around  $t_{NB}$ . Unfortunately for all discharges displayed in Fig.2 the data



available from the LIDAR and ECE diagnostics do not allow concluding that, outside measurement uncertainties, differences in the kinetic profiles should be correlated to changes in  $\beta_N$ . However this circumstance is reasonable, as all discharges considered in the statistics were rigorously performed operating with same parameters of plasma density, current, magnetic field, etc., and only some difference occurred in the initial level of recycling.

Therefore, in order to illuminate the complex mechanism determining the phenomenology that links the initial level of recycling to confinement performance in H-mode, we have extended the analysis including further data of experiments performed with more marked differences in the initial conditions. Moreover we show the impact of the recycling on the kinetic profiles in the scrape-off layer (SOL).

In the next section we show modelling data that allow assessing that changes in the recycling level are accompanied by changes in the temperature occurring

Moreover, in Sec.4 we examine plasma discharges in the same plasma configuration of the experiments taken considered in the present section, but with a more marked difference in the initial conditions, not necessarily of recycling. We will compare plasmas that have, before initiating the main heating phase, a different q-profile due to the use or not of LHCD in prelude, as well as plasmas with LHCD in prelude and slightly different initial conditions of recycling and plasma density. Similarly to the case of plasmas shown in Fig. 2, these experiments, by using some different initial conditions, obtained evident differences in the evolution of the confinement performances in H-mode. Therefore, to extend the analysis to these experiments would be useful to illuminate the complex phenomenology described here. Moreover, it would help determining a key parameter that, influenced by the initial level of recycling, would in turn affect the confinement performance evolution in H-mode.

### 3. ROLE OF RECYCLING IN EXPERIMENTS PRESENTING A HIGH $\beta_N$ PHASE

The link of initial condition of recycling and confinement performance in H-mode, occurring in the phenomenology described in the previous section, has suggested reconsidering previous experiments and their modelling in a new light. We focus here on the experimental aspect.

The experiments considered in the present paper were aimed at developing regimes of high  $\beta_N$  relevant for SS scenarios of ITER [8–11]. Figure 3 summarises the best discharges (performed with  $I_p = 1.5\text{MA}$ ,  $B_T = 2.3\text{T}$ ) in terms of a longer high  $\beta_N$  phase (namely  $\beta_N \approx 2.8$ ,  $H_{98} \approx 1.05$  in ELMy H-mode phase) [8–10].

In developing on JET TB plasmas with high  $\beta_N$ , targets for the main heating power with a lower recycling were produced by operating with a larger radial outer gap (ROG) at around the time  $t \sim \bar{t}_{NB}$ . The lower recycling is the consequence of the reduced plasma interaction with the walls of the main vessel [17,13–15,7]. Figure 4 compares a high  $\beta_N$  discharge (70069) of Fig.3 with a previous reference Pulse No: (68927) performed with a smaller ROG ( $\sim 4\text{cm}$ ). For the former discharge, the  $D\alpha$  levels from the main vessel are slightly lower, Figs. 4a,b, and a bit lower for the

channel looking at high field side of divertor, Fig.4c, consequence of the larger ROG This kind of operation, producing a lower recycling level at  $t \sim t_{NB}^-$ , was maintained in the experiments that were aimed at developing on JET ITER relevant SS scenarios.

The main heating phase of the considered experiments of JET is produced with about 20MW of NB and 2MW of ICRH, applied after the end of the plasma current ramp-up prelude phase. For Pulse No's: 70069 and 76516 of Fig.3, the prelude phase had only an ohmic heating (ohmic prelude), but for Pulse No: 72596 some LH power was utilised for driving non-inductive current during prelude. This operation was carried out for producing a different q-profile at the beginning of the main heating phase.

An extensive search was performed for testing possible improvement of performance in H-mode by means of LH prelude. Consequently, the main heating phase was characterised by absence of a high  $\beta_N$  phase, however testing the effect of different coupled LH power levels and  $n_{||}$  antenna spectra ( $n_{||}$  is the wavenumber component in the direction parallel to the confinement magnetic field).

Conversely, in the discharge of Fig.3 with LH prelude (Pulse No: 72596), a high  $\beta_N$  phase occurred instead by means of less gas fuelled in prelude than in discharge utilised as reference (Pulse No: 70068). The aim of the latter operation was to produce a target for the main heating power with lower density, higher temperature (also at the periphery, see hereafter in the text). Moreover, a lower recycling than in the reference discharge was obtained as shown in Fig.5. The less gas in prelude did not produce significant delay ( $\sim 100$ ms) in the L-H mode transition time: consequently, a desired ELMy H-mode phase was regularly produced [10], see Fig.5c and 6f (described hereafter). Therefore the confinement performance obtained can be compared indeed, as done in Fig.3. As the performance Pulse No: 72595 of Fig.3 was obtained by a suitable gas fuelling in prelude, the obtained improved performance suggested the need of producing targets with lower recycling but also same density, in order to individuate a clear role of the initial recycling condition in determining confinement performance in H-mode. The use of the technique of early gas fuelling overshoot, mentioned in Sec.2, helped assessing this issue in the statistics related in the previous section.

Regarding the use of LH power coupled during the main heating phase, this power did not ever produce, in the considered plasma configuration, current drive effects in the core, as LH waves were fully deposited at the edge [6]. It was the consequence of the relatively high plasma density at the edge and periphery that typically occurs in the main heating phase of plasmas shaped at high triangularity. Unfortunately, the method assessed on FTU for enabling the occurrence of LH effects also at markedly higher density [7] was still not available at the time of the considered experiments of JET.

Figure 6 shows the time evolution of the main plasma parameters of the aforementioned two discharges (Pulse No's: 72595 and 70068) performed with LH prelude. Due to the different gas fuelled in prelude, at the switch-on time of the main heating power ( $t_{NB}^- \approx 3.3$ s), see Fig.5e, discharge 72595 has lower density (Fig.6a), higher electron temperature (Fig. 6b) and markedly lower  $D\alpha$

levels than the reference discharge (Pulse No: 70068). As desired for the experiment, also a higher electron temperature occurs at the periphery, see Fig.6e, which is reasonably due to the less gas fuelling (Fig.5e) and lower recycling (Fig.5a–d).

A phase with a high  $\beta_N$  (in the range 2.5–2.8, Fig. 6c) occurs in Pulse No: 72595, despite the NB power is 5% less than in reference discharge (Pulse No: 70068). The high  $\beta_N$  ( $>2.3$  i.e., the level during H-mode phase without confinement improvement) occurs in the late H-mode phase (for  $t \geq 8.2$ s) and persists for more than 1s for all the time in which the NB power flat top is maintained, see Fig. 6g. Indeed, at the NB switch-off time point ( $t=9.2$ s), the  $\beta_N$  is about 2.5 and strong MHD event occurs only (at  $t=9.3$ s) when the NB power is falling off.

Incidentally, in Pulse No: 76516 of Figure 3 a different initial condition was utilised consisting in a prelude phase with a plasma current ramp with an overshoot in the early phase of discharge (see Fig 3a). This technique, aimed at optimising the q-profile evolution [19], has also the effect of producing a higher ohmic heating before initiating the main heating phase. Consequently, the plasma is transiently more heated, especially at the plasma edge, which is similar to the effect produced by a lower recycling.

In summary, in developing SS scenarios on JET relevant for ITER, all the performance experiments of Figure 3 utilised operations with initial conditions producing lower recycling and higher temperature at the plasma edge. Considering the result of the statistics shown in Sec. 2 these condition would have reasonably helped the achievement of the confinement performances.

#### **4. PARTICLE RECYCLING FROM THE VESSEL WALLS AND TEMPERATURE AT THE PLASMA EDGE**

It is well assessed that operating with lower particle recycling from the vessel wall, higher temperature at the edge occur, consequence of the lower radiation loss from the plasma edge [17]. However, as an example of this effect, we present here some available data of the modelling performed taking into account the parameters of AT experiments of JET [7,8], which were considered at the beginning of the study on JET of the phenomenology linking initial condition of recycling and TB behaviour [13,14].

Transport modelling has been carried out by the EPIT code [20]. The transport along field lines is assumed to be classical and transport coefficients follow from the 21-moment Grad approximation [21,22]. The radial transport is assumed to be anomalous with prescribed radial transport coefficients. All ion species have the same temperature  $T_i$ , which can be different from the electron temperature  $T_e$ . The dynamics of deuterium and impurity neutrals in the SOL is described by an analytical model, which accounts in a self-consistent way for recycling of plasma ions as well as for sputtering processes at the target plates. In the present analysis the effect of impurities has been neglected and only deuterium plasma has been considered. The analysis has been performed in the slab geometry, neglecting the real curvilinear structure of the magnetic field in the SOL of the JET

tokamak, meaning that  $h_x = h_y = \sqrt{g} \equiv 1, \sqrt{g}$ ,  $h_x, h_y$  are metric coefficients). In order to account for the magnetic flux tube expansion in the divertor, we have assumed that the pitch angle changes in the divertor according to the following formula:

$$\begin{aligned} h_\theta(x) &= \left(\frac{B_\theta}{B}\right)_{separatrix} \left(0.5 + 0.5 \frac{x_{plate}}{x_{plate}} \frac{x}{x_s}\right) \text{ for } x > x_s \\ h_\theta(x) &= \left(\frac{B_\theta}{B}\right) \text{ for } x < x_s \end{aligned} \quad (1)$$

where  $x_s$  is the poloidal position of the x-point. The power flowing to the SOL has been estimated as  $P_{SOL} = 16\text{MW}$ . The anomalous radial transport is determined by the coefficients  $D^i = 0.1\text{m}^2/\text{sec}$ ,  $\eta_y^i = 0.2m_i n_i D^i$  and  $\chi_y^e/n_e = 2.5 \chi_y^i/n_e = 10D^i$ . In all calculations the input particle flux to the SOL  $\Gamma_{imp} = 3 \cdot 10^{21} \text{sec}^{-1}$ .

Boundary conditions used in our calculations are shown in Fig.8 where also the computational domain and the numerical mesh are presented. At the core interface constant input energy and particle fluxes as the boundary condition are specified. We assume that all radial gradients are zero at the interface with the private region (PR). Density and temperature decay lengths are used as boundary conditions at the wall. The Bohm condition is used at the divertor plate: the flow velocity at the plate equals to the poloidal projection of the sound speed:  $v_{ix} = h_\theta c_s$  and the energy fluxes are given by  $q_{ex} = \delta_e n_e v_{ex} T_e$ ,  $q_{ix} = \delta_i n_i v_{ix} T_i$ , where  $c_s$  is the sound speed and the energy transmission factors  $\delta_e, \delta_i$  are calculated according to the Igitkhanov model [26].

In the case of deuterium two groups of neutrals are considered: fast and slow neutrals ( $N_D = N_{fD} + N_{sD}$ ). The profile of deuterium atoms is prescribed by a product of exponential functions:

$$N_D^{f,s}(x,y) = N_{f,s}^{plate} e^{-\frac{|x_{plate}-x|}{x} \frac{f,s}{x}} e^{-\frac{(y_M-y)^2}{y} \frac{f,s}{y}} \quad (2)$$

The deuterium neutral densities at the target plate depend on the recycling coefficient R:

$$\int_{VOL} N_D(x,y) \alpha_i^D(x,y) n_e(x,y) dV = R \int_{plate} n_i v_x^i(x_{plate},y) dS \quad (3)$$

where VOL is the volume of the boundary layer and R is an external parameter in the SOL model. It is assumed that the velocity of the neutrals equals to the ion velocity for fast neutrals and it is equal to the thermal velocity in the case of slow neutrals.

The influence of the recycling coefficient on the plasma parameters in the SOL has been investigated. The recycling coefficient was changed from  $R_c = 0.95$  up to  $R_c = 0.99$  and corresponding changes to the total plasma flux to the target plate are  $\Gamma_{plate} = 6 \cdot 10^{22}$  to  $30 \cdot 10^{22} \text{sec}^{-1}$ . The results are summarised in Figure 9.

It is evident that higher plasma recycling leads to the increase of the plasma density and pressure and reduction of the plasma temperature. This effect is relatively strong close to the divertor plate

strike point. For a decrease of the  $D\alpha$  radiation of 20%, a decrease of the recycling coefficient ( $R_c$ ) of about 25% occurs,  $P_{\text{rad-D}\alpha} \propto 1/(1 - R_c)$ . The temperature profile in Figure 8 shows that, for low recycling operation, the most marked enhancement of  $T_e$  is expected to occur in the deeper radial region of SOL, i.e., at  $r \sim 1$ . The temperature at this layer will be referred to as  $T_{e\_edge}$ . A decrease of the  $D\alpha$  radiation of 20% gives an increase of about 40% of  $T_{e\_edge}$ . Consequently, a more marked increase of  $T_{e\_edge}$  should be expected to occur with the reduction of about 30%, which has been assumed at the end of Sec.2 for producing a marked increase of  $\beta_N$  ( $\sim 20\%$ ) in the considered AT scenario.

The link between the level of recycling,  $T_{e\_edge}$ , and  $T_{e\_periphery}$  (i.e. in the layer  $\rho \approx 0.8 - 1$ ) is consistent with data of Figure 6, in which two regimes of gas fuelling in prelude produce targets with different density, recycling and also  $T_{e\_periphery}$ , see Fig.6f (although the confidence is not within the uncertainty of measurement). As referred in Sec.2, preliminary results of experiments on JET supported by the HRTS (High Resolution Thomson Scattering) diagnostic measurement seem assessing the link between the level of recycling,  $T_{e\_edge}$ , and  $T_{e\_periphery}$  in prelude.

## 5. MODELLING OF THE PLASMA CURRENT PROFILE EVOLUTION, TRANSPORT AND STABILITY

The results of Sec.2, supported by data of Sec.3 connect the level of recycling occurring before the NB switch-on time to the confinement performance in H-mode. In this section, the evolution of the radial profiles of current density and magnetic shear, as well as transport and stability are assessed. As discussed in the next section, the related results help illuminating the complex phenomenology described in Secs.2 and 3.

We focus here on the features of TBs occurring in discharges aimed at developing AT scenarios for ITER [7–9]: for a certain discharge, we compare the respective phases of high  $\beta_N$  and standard H-mode. Moreover, the time window of two discharges, respectively, exhibiting or not a high  $\beta_N$  phase has been considered for comparison.

We compare the high  $\beta_N$  performance Pulse No: 70069 (of Fig.3), with purely ohmic prelude, with discharge 70068 with LH prelude (the latter discharge has been considered as reference also for the experiments of Fig.6). For this couple of discharges, the time evolution of the main plasma parameters is shown in Fig.10. Only Pulse No: 70069 presents a high  $\beta_N$  phase (Fig.10e) that terminates at the onset of strong MHD event (mode 2/1), see Fig.10f. Due to the LH power coupled in the prelude phase, in Pulse No: 70068, a target for the main heating power with deeply reversed q-profile is expected to occur, as consequence of non-inductive current driven in the core. As discussed in Sec.3, Pulse No: 70068 of Fig.10 belongs to a series of experiments in which the achievement of high  $\beta_N$  was prevented by strong MHD event occurring too early. Consequently, before having obtained the new successful result with LH prelude (consisting in Pulse No: 72596 of Fig.3 and Fig.6), the LH prelude was not considered a tool useful for producing well-confined and stable plasmas for developing the considered AT scenarios.

The kinetic profiles occurring during the high  $\beta_N$  phase (at  $t = 6.0\text{s}$ ) and after its termination (at  $t = 7.0\text{s}$ ) for Pulse No: 70069, and during H-mode (at  $t = 6.0\text{s}$ ) for Pulse No: 70068 are shown in Fig. 11. In order to model the evolution of the radial current density profile and perform transport analysis, the following approach has been utilised.

The model of neoclassical resistivity (NCLASS) and the Faraday equation contained in the JETTO code [23] are used to determine the current diffusion in the plasma column by taking into account the kinetic profiles, the effective ion charge and the EFIT [24] equilibrium reconstructed using magnetic data.

The density profiles (Fig.11a) have been assumed to have the same steep gradient within the uncertainties of the two LIDAR and the interferometer diagnostic systems. This choice overestimates the gradient in case (Pulse No: 70068) a slightly lower density is reached during H-mode phase, thus allowing a more confident comparison of the  $j_{BS}$  profiles occurring in the compared experiments. For Pulse No: 70069, during the high  $\beta_N$  phase, a slightly higher pedestal density ( $\sim 10\%$ ) occurs indeed, as shown in Fig 11a, while  $T_{e\text{-periphery}}$  (at  $\rho \sim 0.8$ , Fig.11b) is slightly higher (of about 20%) than after the high  $\beta_N$  phase termination. After that time,  $T_{e\text{-periphery}}$  is reduced to a value close to that occurring in Pulse No: 70068 that does not present a high  $\beta_N$  phase. A significant effect of the electron temperature at the periphery in locally enhancing  $j_{BS}$  for Pulse No: 70069 is thus expected to occur, due to the contribution of the term  $T\nabla n$  in the relation 4 [1]:

$$j_{BS} \propto T\nabla n + 0.04nn\nabla T \quad (4)$$

In the JETTO code, the complete expression of the bootstrap current is utilised [25]. Incidentally, an analysis of the current drive in the experiments in Refs. 7,9 was also performed utilising the TRANSP code [26], but this work did not include the available data of plasma periphery as done instead in the present paper ( $\rho \sim 0.9$ ).

In case with LH power utilised in the experiment, the correspondent deposition profile is calculated with the LHstar code, which includes the wave physics of the plasma edge and periphery [27,28,6]. The EFIT code also provides the current density profile in the very early phase of discharge ( $t \sim 1\text{s}$ ), which is used as the initial condition for the JETTO simulation.

Figure 12 shows some results of the plasma current profile evolution. Fig.12a tests, for Pulse No: 70069 of Fig.10, the q-profile evolution during the H-mode phase modelled by JETTO with that provided by EFIT using magnetic input data constrained by motional stark effect (MSE) measurements, and general agreement is found. Moreover, the q-profile modelled with JETTO shows a local flattening during main heating phase ( $t = 6.0\text{s}$ ) at large radii ( $\rho \sim 0.90$ ), which indicates the occurrence of a region of low magnetic shear. Conversely, a similar analysis performed for Pulse No:70068 of Fig.10 shows that the flattening of the q-profile at large radii is much less pronounced than in case of Fig.12a. Unfortunately, the EFIT reconstruction method and MSE measurements used to determine the q-profile do not allow a precise determination of such a feature localised in this region of plasma. The utilised approach for modelling the q-profile evolution, which includes the available data of kinetic profiles

at the plasma periphery, provides a useful tool for properly considering, in the realistic context of the experiment, also local effects of the magnetic shear on transport.

For the same discharges of Fig.10, the q- and shear- profiles at a time point ( $t = 3.5s$ ) just after the main heating power switch-on are compared in Fig.12b,c. This comparison is useful for assessing the role of different initial conditions in the compared plasmas. For the case with LH current drive prelude (Pulse No: 70068) a deeply reversed q-profile is obtained Fig.12b, as expected. Moreover, the magnetic shear at large radii is markedly higher ( $s \approx 1.5$  against  $s \approx 0.6$ ), see Fig.12c.

Therefore, an important result is that the plasma with LH prelude represents a target, for the main heating power, which is farer from the condition of low magnetic shear at large radii than the one with purely ohmic prelude. The shear at large radii ( $s \approx 1.5$  at  $\rho \approx 0.85$ ), Fig.12c, is markedly higher than in the case with purely ohmic prelude ( $s \approx 0.6$  at  $\rho \approx 0.85$ ), consequence of the negative shear produced in the core. This undesired conditions is related to the deeply reversed q-profile occurring in the case with LH prelude, Fig.12b, as the LH current is mostly driven in the inner radial half of plasma, due to the radially narrow Te profile target ( $T_{e0} \approx 4.5keV$ ,  $T_e \approx 2keV$  at  $\rho \approx 0.35$ ) occurring in prelude. The LH current density calculated with the LHstar code [27,28,6], considering the plasma parameters of Pulse No: 70068, is:  $j_{LHpeak} \approx 5 \cdot 10^6 m^{-3}$  at  $\rho \approx 0.35$ , and  $j_{LH} \approx 2 \cdot 10^6 m^{-3}$  at  $\rho \approx 0.40$ .

Transport analysis has been performed considering one of the AT Pulse No: 70069 of Fig.10. The two phases of H-mode are compared, respectively, during (at 5.5s – 6.0s) and after (at 7.3s – 7.8s) the high  $\beta_N$  phase, see Fig.10e. The radial profiles of the electron and ion thermal conductivities are shown in Figure 13. During the high  $\beta_N$  phase, the electron conductivity is markedly lower (more than a factor two) in the whole radial region  $\rho \approx 0.6$ , and slightly lower (30%) more externally (up to  $\rho \approx 0.8$ ). The ion conductivity presents less pronounced differences: it is 40% lower for  $\rho \leq 0.5$  and 20% for  $\rho \leq 0.8$ . Consequently, the high  $\beta_N$  phase is characterised by a radially large TB. We show now the radial profiles of the plasma current density and magnetic shear for the discharge (Pulse No: 70069) with high  $\beta_N$  phase of Fig.10. Figure 14 displays the contributions of the NB power and the bootstrap effect at two different time points, respectively, before (at 6.0s) and after (at 7.3s) the high  $\beta_N$  phase termination. The magnetic shear radial profiles are shown in Fig 14b in way useful for evidencing large plasma radii. Two couples of time points are considered, respectively, before (at 5.0s and 6.0s) and after (at 7.3s and 8.0s) the high  $\beta_N$  phase termination.

A low shear ( $s \approx 0.2 \pm 0.02$ ) thus occurs at large radii ( $\rho \approx 0.92 \pm 0.02$ ) during the high  $\beta_N$  phase of the considered AT discharge.

A stability analysis has been carried out using the ideal MHD code MISHKA-1 [29] considering the main heating phase of discharges of Fig.10. The equilibria for the same plasma discharge of Fig. 10 have been reconstructed from the current density and pressure profiles derived from JETTO simulations. These profiles, together with the fixed boundary shape of the last closed flux surface are supplied to the HELENA code [30], which produce the static equilibrium employed by MISHKA-1. The plasma is found to be stable to infinite-n ballooning modes at the low magnetic shear generated by the strong bootstrap current, see Fig. 14a. However, the plasma discharge (Pulse No: 70069) with

a high  $\beta_N$  phase has a bigger margin of stability minimum shear at the plasma periphery ( $\Delta s_{\min} \approx 4.0$ ,  $\beta_{N\max} \approx 2.8$  for Pulse No: 70069) than the plasma with lower  $\beta_N$  ( $\Delta s_{\min} \approx 2.3$ ,  $\beta_{N\max} \approx 2.6$  for Pulse No: 70068).

Considering discharges of Fig.6, a stability analysis of the plasma edge and during prelude has been performed using the GENE code [31]. For the parameters of discharge (Pulse No: 70068) with higher density and lower temperature, during the L-mode phase there are unstable ETG modes, while they are much weaker (but still slightly unstable) for the compared discharge (Pulse No: 72595). Simulations aimed at assessing the non linear behaviour of turbulence are in progress and full results will be presented in a dedicated work.

It is worth noting that the modelling of the current drive was performed considering several time points (about ten) during and after the collapse of the high  $\beta_N$  phase. Consequently, the relatively high bootstrap current fraction and low shear of Pulse No: 70069 of Fig.14 is representative of the behaviour of the high  $\beta_N$  phase since its build-up (at  $t \approx 4s$ ), as kinetic profiles at the periphery are similar to those displayed in Fig.11.

These circumstances suggest that initial condition of lower shear (Fig.12b) would favour the build-up of an improved confinement phase that, in turn, produces higher temperature at the periphery since the beginning of the main heating phase. In analogous way, initial conditions of low recycling, favouring the occurrence of higher temperature at the edge and periphery, would also help the build-up of a higher bootstrap current fraction and initial condition of low shear at large radii.

In the next section we propose some ideas that help illuminating the described complex phenomenology, which seems linking together initial conditions of low recycling (discussed in Sec.2) and magnetic shear (discussed in the present section) to the build-up of improved confinement in H-mode.

## 5. INTERPRETATION OF THE PHENOMENOLOGY

We propose here an interpretation of the phenomenology shown in Sec.2, and Sec.3, which show that initial conditions of recycling and magnetic shear at large radii are linked to the achievement of confinement performance in H-mode. Due to the intrinsic complexity of the phenomenology, we do not pretend giving a fully exhaustive explanation but only proposing some ideas that help illuminating the phenomenology and addressing a more complete search on the related issue.

The plasmas considered here have an H-mode phase that starts just after the end of the current ramp-up; consequently, the current is not fully relaxed as shown by the q-profile evolution of Fig.12a. The H-mode develops a phase with high values of  $\beta_N$  and H-factor ( $\sim 1.1$ , see Fig.3). This phase is maintained for several confinement times, until strong MHD event occurs. In some cases utilising LH prelude (e.g., in Pulse No: 72595 of Fig.6) the high  $\beta_N$  develops late in H-mode and strong MHD event occurs only after the main heating power has been switched-off. As shown in Sec.3, in the considered conditions, no data are available documenting that more stable and well-confined H-mode plasma can be produced operating with lower temperature at the periphery, lower recycling and higher density in prelude phase with respect to performances of Fig.3.



These high  $\beta_N$  regimes are accompanied by radial profiles that present relatively high electron temperature and bootstrap current density, and low magnetic shear ( $s \approx 0$ ) at the periphery ( $\rho \sim 0.8 \div 0.9$ ). Moreover, they are favoured by operations that produce a lower  $D\alpha$  level in the prelude phase, before the NB power switch-on time point, as demonstrated in Sec.2. Signatures suggesting the possible occurrence of the related phenomenology were present in the experiments summarised in Sec.3. As shown by Ref. 17 and modelling results of Sec.4, these low recycling regimes are characterised by a relatively high temperatures at the edge.

Stability analysis of the plasma edge and periphery shows that more stable plasma occurs in L mode in case of higher temperature at the edge and periphery. Global stability analysis performed for the H-mode phase indicates that a lower shear at large radii would help stability and confinement. Reasonably, the related phenomenology would link parameters of the plasma edge (recycling and temperature) and periphery (temperature, bootstrap current density, shear) in L-mode that, in turn, are connected to H-mode confinement performance in the core. This link suggests that a sort of virtuous loop, involving the parameters at the edge and periphery, would act and tend sustaining the high  $\beta_N$  phase. The hypothesised feedback mechanism is favoured by initial conditions of low recycling, high temperature of the edge and periphery and low magnetic shear at large radii, as described hereafter.

High temperature at the edge favours the occurrence of higher  $T_{e\text{-periphery}}$  that, in turn, promotes the occurrence of high  $j_{BS\text{-periphery}}$  (by the term in the expression 4) and low  $s_{\text{periphery}} \approx 0$  in building H-mode profiles consistent with current drive data of Fig.14. The relatively high  $T_{e\text{-periphery}}$  observed in these regimes should be the consequence of turbulence stabilisation that improves confinement via low local shear, favoured by a more stable initial condition of plasma in L mode, as supported by the GENE code results.

In summary, high  $T_{e\text{-periphery}}$  drives higher  $j_{BS\text{-periphery}}$  that promotes the  $s_{\text{periphery}} \gg 0$  condition to be further approached and maintained. In this way, the feedback loop would work and favour, via confinement improvement, the occurrence of further higher  $T_{e\text{-periphery}}$ . Such feedback would tend stabilising the system by leading the plasma close to the limit of neoclassical transport. The occurrence of some shear increase, detrimental for confinement, could be compensated by a proper self-adjustment of the pressure profile steepness, producing a higher  $j_{BS\text{-periphery}}$  sufficient for maintaining the shear low and keeping the system close to the limit of neoclassical transport [32]. In this sense, higher  $T_{e\text{-periphery}}$ , promoted by low recycling conditions at the beginning of the main heating phase, would help activating the feedback effect. This might explain the link between conditions near the end of the L-mode phase and during H-mode phase. Since the condition  $s_{\text{periphery}} \approx 0$  favours the occurrence of high  $T_{e\text{-periphery}}$ , once reached, it could be in principle self-sustained in steady-state. Unfortunately, such control mechanism would work in the framework of two opposite effects of high  $j_{BS\text{-periphery}}$ : one favourable, via stabilizing ballooning modes due to low local shear, the other, detrimental, as it helps destabilising low-n MHD modes in high  $\beta_N$  plasma [33]. Since the non-inductive current occurring in the experiment is not sufficient for fully freezing the current

relaxation, the magnetic shear tends naturally increase at the plasma periphery: consequently the plasma tends to loose the ballooning stability condition ( $s \approx 0$ ). When reached such phase of the current diffusion, in trying restoring the low shear condition, the feedback would produce steeper and steeper pressure gradients but, when a certain threshold in steepness is exceeded, the onset of low- $n$  MHD modes occurs, leading to the TB collapse and the high  $\beta_N$  phase terminates. This picture is consistent with the phenomenology of the high  $\beta_N$  experiments shown in Fig.6 and Fig.10.

Incidentally, the hypothesised feedback mechanism has some analogy with an explanation of the ELM activity via  $j_{BS}$ , which produces opposite conditions at the edge for the occurrence of the peeling and ballooning modes [34]. However, in the present context, as found by transport analysis, the TB penetrates radially deeper in the plasma periphery than in a simple H-mode.

On the basis of the proposed hypothesis and the results shown in the paper, we can now propose an interpretation of the phenomenology of the high  $\beta_N$  phase. This phase manifests as a radially broad TB provided that proper initial conditions (at  $t \sim t_{NB}^-$ ) occur at the edge and periphery ( $\beta \sim 0.8 - 1$ ). Namely, the high  $\beta_N$  phase occurs in discharges 72595 (with LH and less gas in prelude, see Fig.6) and 70069 (with ohmic and standard gas prelude, see Fig.10), but not in the discharge used as reference in both figures 70068 (with LH and standard gas in prelude).

The AT reference Pulse No: 70069 of Fig.10 would present a high  $\beta_N$  phase since the plasma target of the main heating power (at  $t \sim t_{NB}^-$ ) has a lower magnetic shear at large radii (Fig.12b red line), than in the compared discharge without high  $\beta_N$  phase (Fig.12b blue line). The AT reference PulseNo: 72595 of Fig. 6 would present a high  $\beta_N$  phase since the plasma target at  $t \sim t_{NB}^-$  has higher temperature also at the periphery (Fig.6e and analysis of Sec.4), which promotes a high bootstrap current density fraction at the periphery, via Eq.4. The higher temperatures at the periphery are the effect of the less gas fuelled in prelude (Fig.5b) than in discharge (70068) without high  $\beta_N$  phase. The loop favouring the confinement improvement would be thus activated by initial conditions (at  $t \sim t_{NB}^-$ ) that occur at the edge and periphery. These conditions consist in a relatively low magnetic shear and a high temperature at the periphery. The onset of MHD event would be the consequence of the too steep pressure gradient that would be necessary for restoring a low transport condition, when the shear at the periphery tends increasing for current diffusion. This hypothesis is consistent with the phenomenology of Fig.6 and Fig.10, as well as with the statistics in Sec.2 and turbulence in L-mode, current drive, transport and global stability analyses.

## 6. COMMENTS AND CONCLUSIONS

Low recycling operations produced in the L-mode (prelude) phase, before the occurrence of H-mode (main heating) phase, in experiments of JET aimed at developing ITER-relevant AT scenarios, favour the occurrence of a high  $\beta_N$  phase in H-mode. This phase is sustained for several confinement times and ceases at the onset of strong MHD.

The effect of initial lower  $Da$  levels on the occurrence of a high  $\beta_N$  phase is evidenced by experiments performed with same operating parameters, in which different initial  $Da$  levels were

produced, shot by shot, by means of different gas fuelling waveforms, which however guaranteed the production of the same target density. Moreover changes occurring randomly during the experimental session were also monitored. Accurate statistics shows that the averaged change of all the available  $D\alpha$  level signals measured before starting the main heating phase is linked to the  $\beta_{N\_max}$  value occurring in H-mode phase.

We have analysed the features of TBs, occurring in the related experiments, considering three reference discharges performed in the same plasma configuration. Two of them presented a high  $\beta_N$  phase (defined in Sec.3) and they were produced, respectively, with ohmic and LH prelude. The third one was performed with LH prelude but it did not present a high  $\beta_N$  phase. In the latter case, the onset of strong MHD produced too soon the TB collapse. On the basis of modelling results, the comparison of the aforementioned three discharges has allowed formulating a hypothesis on the link between edge/periphery conditions in L-mode and confinement performance in H-mode.

Analyses of turbulence of the edge, transport current drive and MHD stability have been produced for the mentioned reference discharges. We have made comparisons at two time windows of a same discharge, respectively, during the high  $\beta_N$  phase and after its termination. Moreover, we considered a certain time of two comparable discharges that, respectively, presented or not a high  $\beta_N$  phase, due to some different conditions in prelude.

Modelling in L-mode phase shows that a weaker turbulence occurs in discharge performed with less gas, lower recycling and higher temperature at the periphery. Available modelling data show that the high  $\beta_N$  phase is accompanied by high  $J_{BS}$  especially at the periphery  $\rho \sim 0.9$ , which locally produces low magnetic shear. The confinement is significantly improved within a large plasma volume ( $\rho \sim 0.8$ ).

Stability analysis of discharges that, respectively, present or not a high  $\beta_N$  phase shows that the confinement performance occurs consistently with a bigger margin of stability minimum shear near the plasma edge than in the case that does not exhibit improvement.

In order to interpret the phenomenology that links initial parameters of the edge and confinement performance, a feedback mechanism has been hypothesised that links together, via the term of relation (4), initial conditions of  $T_{edge}$ ,  $T_{periphery}$ ,  $J_{BS\_periphery}$ ,  $s_{periphery}$  and confinement of the plasma column in H-mode. Following this interpretation, we can conclude that an insufficient current drive would prevent the desired occurrence of a sustained high  $\beta_N$  phase. Indeed, in the considered experiments, the onset of strong MHD event is due to the plasma current that continues to diffuse, despite of the relatively high bootstrap current that occurs during the high  $\beta_N$  phase. On the other hand it is reasonable to assume that a further increase of the bootstrap current, e.g., by utilising higher heating power, would produce pressure gradients too steep and incompatible with stability of detrimental low-n MHD modes. Therefore, the related results of JET indicate that further methods for producing non-inductive current in tokamak plasmas are essential for the progress of AT activities foreseen for ITER.

At this regard, it is important to solve the problem of the lack of penetration of the coupled LH

power in the core, which occurred in experiments of JET [6] having the same ITER-relevant plasma configuration of high triangularity of discharges considered in the paper. Once removed parasitic effects preventing the deposition of the coupled LH power at the edge, by the method in Ref. 7, the LH current drive could efficiently support the bootstrap fraction, thus favouring the sustainment of the high  $\beta_N$  phase. This progress on current drive can be obtained by next experiments, including the ITER-like wall experiments planned on JET, which should take into account the new method for enabling the LH current drive at high plasma densities. This method, based on theoretical prediction [27,28] proved by experiment on FTU [7], requires operations useful for producing relatively high temperature at the edge and periphery, which helps also the formation of plasmas stable and well confined in large volumes as discussed here.

The idea of connecting the recycling to confinement found some support by recent experiments of JET [16]. In the present paper, we have individuated the more specific aspect of the low recycling as an initial condition (in L-mode) for improving performance in H-mode. Such phenomenology was assessed by the AT experiments of JET that concluded years ago the operations in carbon walls. Further tests should be carried out in the next experiments of JET, in particular, in those aimed at developing the Hybrid scenario in ITER-like wall. Such a test could demonstrate that the results found in the present paper would not apply only to a certain specific condition of experiment, but they would have a more general validity and help identifying a possible new regime.

A marked change of the recycling and the temperature at the edge and periphery of a L-mode plasma has been already done in FTU (Frascati Tokamak Upgrade) with several methods, including operations with proper gas fuelling waveforms, and producing plasmas with a larger clearance from the walls, thus reducing the plasma wall interaction with consequent enhancement of the temperature at the edge and periphery [7].

The High Resolution Thomson Scattering (HRTS) diagnostic measurement, now routinely available on JET, enables providing further confident proofs that a relatively high electron temperature at the plasma periphery and a low recycling, considered at a time point just before the NB power switch-on, are key parameters that would determine confinement performance during the H-mode phase. The statistics shown in Sec.2 allows making a prediction for the experiment planned on JET for developing the ITER-relevant Hybrid scenario, which operates in conditions not very different from those of the experiments considered in the paper. A marked decrease of the D level ( $\sim 30\%$ ) produced before the switch-on of the main heating power would determine an evident improvement of  $\beta_N$  ( $\sim 20\%$ ) during the H-mode phase. Preliminary results of experiments aimed at developing the Hybrid scenario in ITER-like wall seem supporting this behaviour. If confirmed, the phenomenology assessed here, for AT discharges of JET performed in carbon wall, would have a more general impact in experiments in ITER-like wall and with different operating plasma current and confinement magnetic field.

## ACKNOWLEDGMENTS

This work was supported by EURATOM and carried out within the framework of the European Fusion Development Agreement. The views and opinions expressed herein do not necessarily reflect those of the European Commission

## REFERENCES

- [1]. Freidberg, J. Plasma Physics and Fusion Energy, Cambridge University Press, 2007
- [2]. J. Garcia and G Giruzzi, “Conditions for the sustainment of high-beta stationary scenarios in tokamaks”, Plasma Physics and Controlled Fusion **54** (2012) 015009
- [3]. J. Garcia, G. Giruzzi, J. F. Artaud, V. Basiuk, J. Decker, et al., “Critical Threshold Behavior for Steady-State Internal Transport Barriers in Burning Plasmas”, Physical Review Letters **100**, 255004 (2008)
- [4]. J. Garcia, G. Giruzzi, Critical Behavior of Magnetically Confined Plasma Regimes, Physical Review Letters **104**, 205003 (2010)
- [5]. Fisch, N.J., “Theory of current drive in plasmas”, Reviews of Modern Physics, **59**, (1987) 175-234
- [6]. R. Cesario et al., Plasma Physics and Controlled Fusion, Volume **53**, Issue 8, pp. 085011 (2011)
- [7]. R. Cesario et al., Nature comms. 15 55 2010
- [8]. J. Mailloux et al, Proc. 34th EPS Conf. On Plasma Physics, Warsaw 2007 P4-151 (2007)
- [9]. X. Litaudon et al., Plasma Physics and Controlled Fusion 49 (2007) B529–B550
- [10]. F. Rimini et al., in Proceedings of the 22nd IAEA Fusion Energy Conference, Geneva, Switzerland, October 2008 EX/1-2 (2008)
- [11]. J. Mailloux et al. 36th EPS Conference on Plasma Physics Sofia, June 29-July 3, 2009 ECA Vol.33E, P-5.164 (2009)
- [12]. F.G. Rimini, et al., Nuclear Fusion **45** (2005) 1481–1492
- [13]. R. Cesario, et al. in Physics of Plasmas, **11** (2001) 4721
- [14]. R. Cesario et al., “Operation with Low Recycling & Observation of Internal Transport Barriers Sustained by Lower Hybrid Current Drive in JET”, EFDA-JET Internal Report PR02, April 2002
- [15]. C. Castaldo, et al., Physics of Plasmas, **9** 8 (2002) 3205
- [16]. E. Joffrin, et al., High Confinement Hybrid Scenario in JET and its Significance for ITER, IAEA Conference Daejeon, Korea Rep.Oct. 2010, EXC/1-1 (2010)
- [17]. Post, D.E. and Behrisch, R., Physics of Plasma-Wall Interactions in Controlled Fusion, NATO ASI Series, Series B, Physics, Plenum Press 1986, New York.
- [18]. S. Brezinsek, et al., Journal of Nuclear Materials **390–391** (2009) 267–273
- [19]. J. Hobirk et al., 36thEPS Conference on Plasma Physics, ECA Vol. 33E 2009) O5.057
- [20]. Zagorski, Journal of Technical Physics **37** (1996) 7

- [21]. Yu.L. Igitkhanov et al., Proc. 14th EPS Conf. on CFPP, Madrid (1987), Pt.II, p.760
- [22]. H.A.Claaßen, H.Gerhauser, R.N.El-Sharif, Report of KFA Jülich, JÜL-2423 Jan.1991
- [23]. G. Cenacchi, A. Taroni, in Proc. 8th Computational Plasma Physics, Eibsee 1986, EPS 1986), Vol. **10D**, 57
- [24]. K. Ida, Plasma Physics and Controlled Fusion **40** (1998) 1492
- [25]. C.E. Kessel, Nuclear Fusion, Vo1.**34**. N0.9 (1994)
- [26]. I. Voitkevovich et al, to be pub. in Nuclear Fusion
- [27]. R. Cesario, et al., Physical Review Letters, **92** 17 (2004) 175002
- [28]. R. Cesario et al., Nuclear Fusion **46** (2006) 462-476
- [29]. Mikhailovskii et al, Plasma Physics Report, **23**, 844 (1997)
- [30]. Huysmans et al, Proc CP90 Conf on Computational Physics, p371 1990)
- [31]. F. Jenko et al., Physical Review Letters. **80**, 4883 (1998)]
- [32]. G. L. Jackson et al. Physical Review Letters **67** 3098 (1991)
- [33]. Greenfield et al PPCF 1993, et al. Plasma Physics and Controlled Fusion **35** (1993) B263
- [34]. S. Saarelma, et al., Plasma Physics and Controlled Fusion **42** 2000) A139–A145

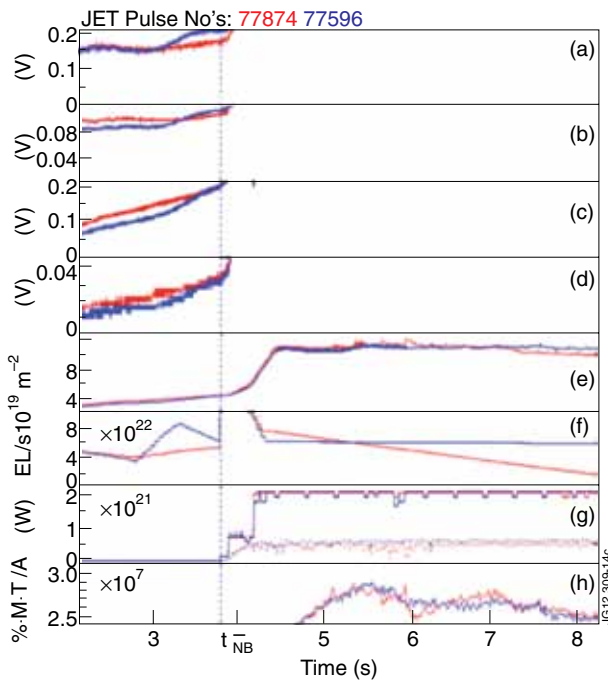


Figure 1: Time traces of some parameters of two AT discharges of JET at  $I_p = 1.8\text{MA}$ ,  $B_T = 2.7\text{T}$ ,  $q_{95} \sim 5$ , plasma shaped at high  $\delta$  ( $\sim 0.4$ ): Pulse No: 77874 (red lines), Pulse No: 77596 (blue lines).  $D\alpha$  signals during late L-mode phase from main vessel in the a) horizontal and b) vertical line of sight, and divertor from the lines of sight in c) low field side and d) high field side. e) Line-averaged plasma density, f) gas fuelling waveforms, g) NB (continuous lines) and ICRH power (dotted lines), h) normalised beta ( $\beta_N$ ).

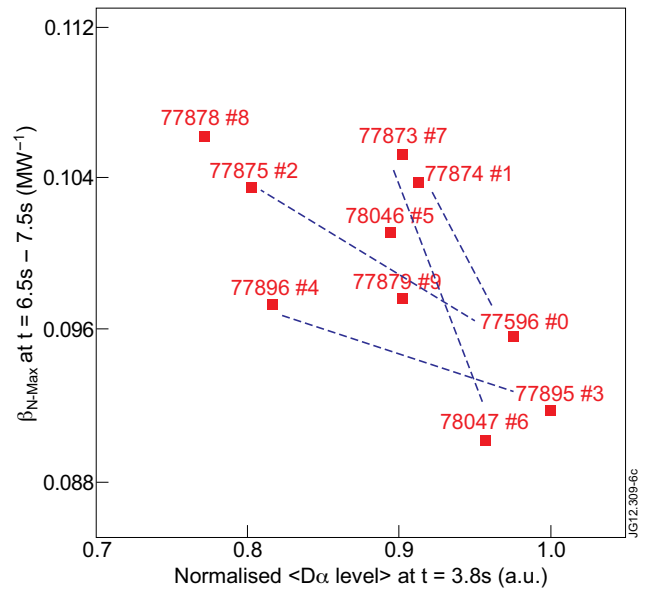


Figure 2: The maximum  $\beta_N$  ( $\beta_{N\_Max}$ ) normalised to the main heating power and kept in a time window from 2.5s to 3.5s after the main heating power switch-on time point is plotted versus the average of the available  $D\alpha$  signals, kept at the time  $t_{NB}$ . The operating main heating power is in the range 25MW – 30MW. The dashed segments link cases with matched main heating power.

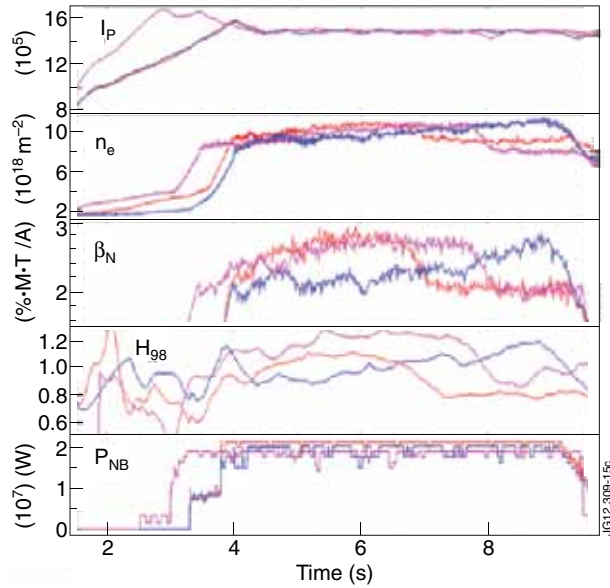


Figure 3: Time traces of JET records  $\beta_N$  for TB plasmas, with plasma shaped with high triangularity ( $\delta \approx 0.4$ ),  $I_p = 1.5\text{MA}$   $B_T = 2.3\text{T}$ ,  $q_{95} \approx 5$ , in experiments aimed at approaching ITER-relevant SS regime. Pulse No's: 70069 (red lines), 72596 (blue lines), 76516 (magenta lines). The LH power waveform utilised in prelude Pulse No: 72596, not displayed, is shown in Fig.6h (blue line).

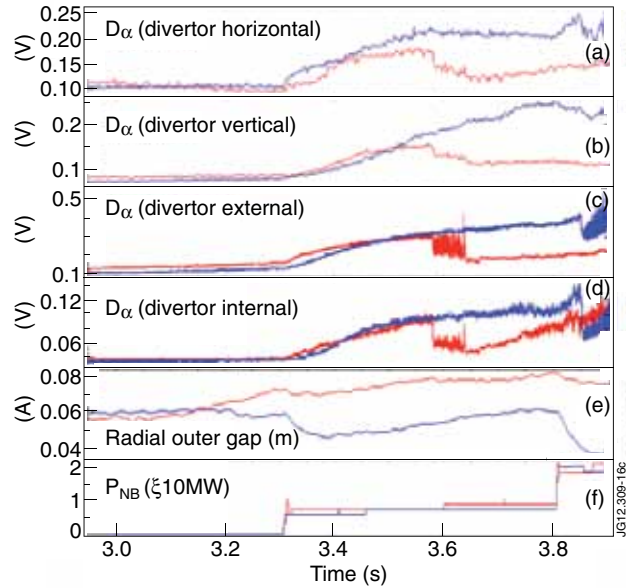


Figure 4: Time evolution at around  $t_{NB}$  for dPulse No: 70069 of Fig.3 (red lines) and for a reference experiment previously produced in the same plasma configuration, Pulse No: 68927 (blue lines).  $D_\alpha$  level from the main vessel lines of sight a) horizontal and b) vertical, divertor c) low field side, d) high field side, e) radial outer gap (ROG), f) neutral beam power.

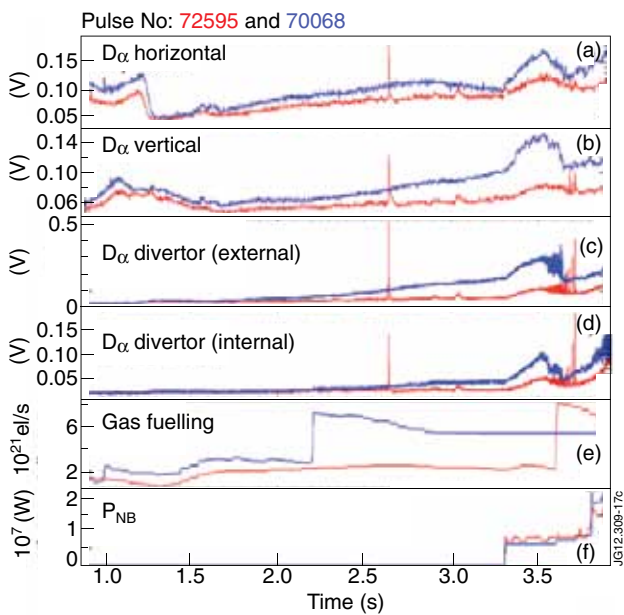


Figure 5. Time evolutions for Pulse No: 72595 (red lines) and 70068 (blue lines). a)  $D_\alpha$  signal from the line of sight in the main vessel a) horizontal and b) vertical, divertor chamber from c) low field and d) high field side, e) gas fuelling waveforms, f) NB power.

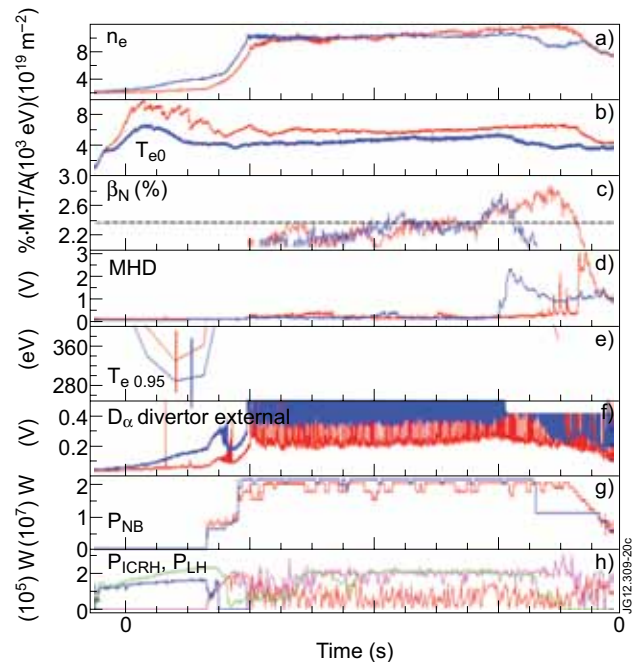


Figure 6. Time traces of the main parameters of Pulse No's: 72595 (red lines in all boxes but in h), 70068 (blue lines in all boxes but in h). a) line-averaged plasma density, b) electron temperature, c) normalised beta, d) MHD (2/1) monitor, (e) electron temperature at the periphery ( $r/a > 0.9$  interpolated from LIDAR and edge-LIDAR), f)  $D_\alpha$  level from the divertor (low field side line of sight), g) NB power, h) LH power: Pulse No's: 72595 (blue line), 70068 (green line), ICRH power: 72595 (red line), 70068 (magenta line).

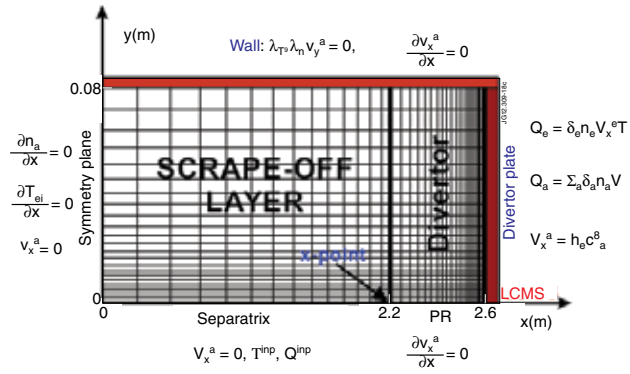


Figure 7: Computational mesh and boundary conditions.

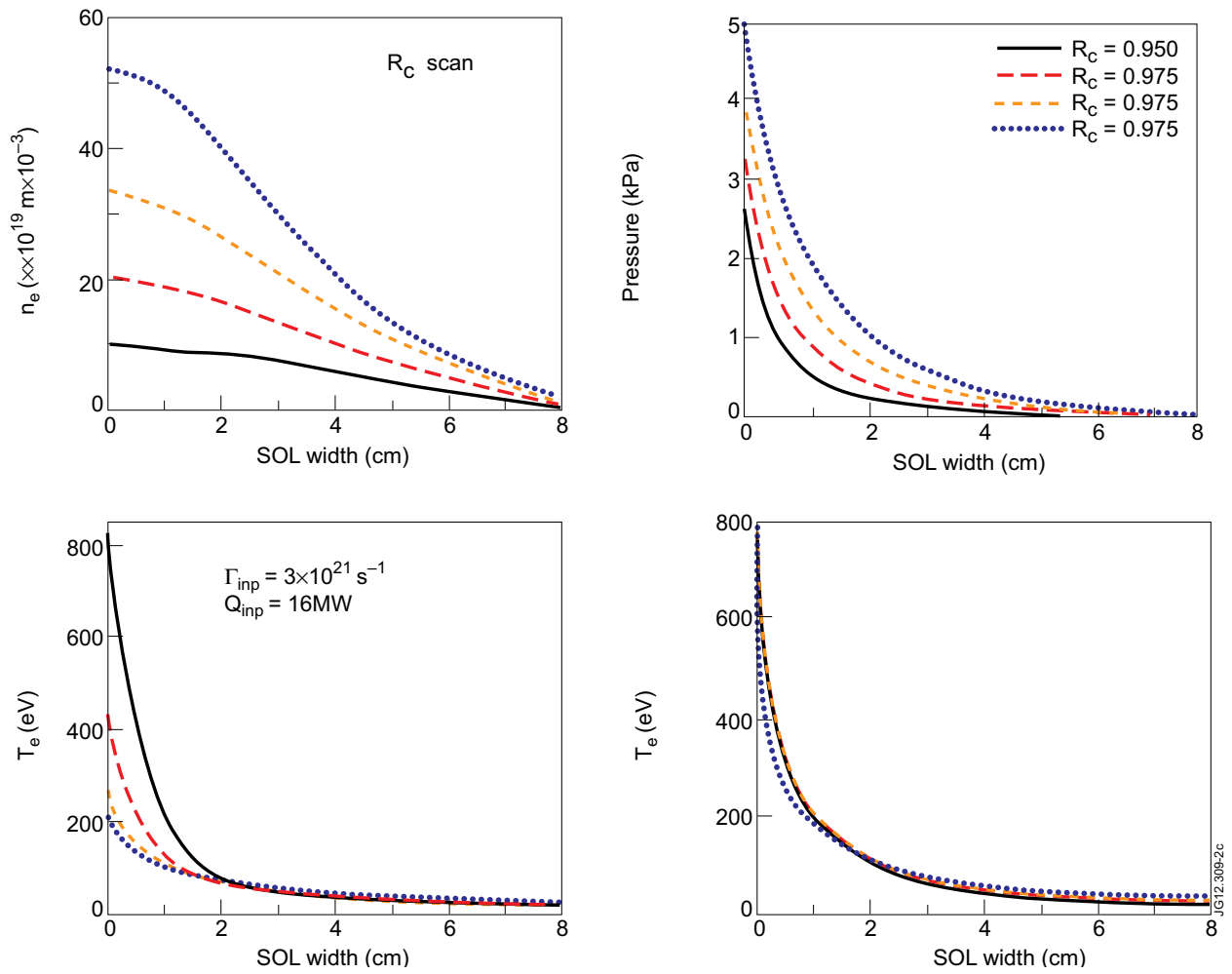


Figure 8: Radial plasma kinetic profiles in the SOL at midplane for different recycling coefficient. Plasma parameters of TB plasma of JET at low triangularity,  $\delta \approx 0.2$ ,  $I_p = 1.5 \text{ MA}$ ,  $B_T = 3.45 \text{ T}$ .



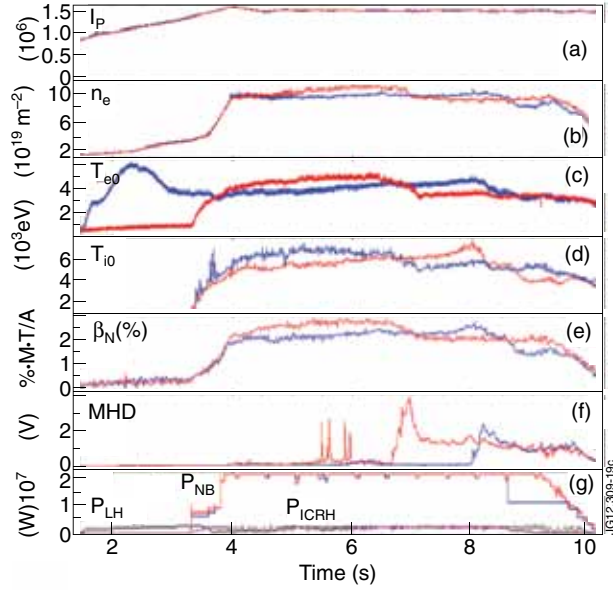


Figure 9: Time traces of the main parameters of two experiments considered in the modelling: Pulse No's: 70069 (red lines), 70068 (blue lines). a) plasma current, b) line-averaged plasma density, central temperature of c) electrons (from ECE), d) ions, e)  $\beta_N$ , f) MHD (mode 2,1), g) NB power, ICRH power: Pulse No's: 70069 (magenta line), 70068 (green line), LH power Pulse No's: 70068 (black line).

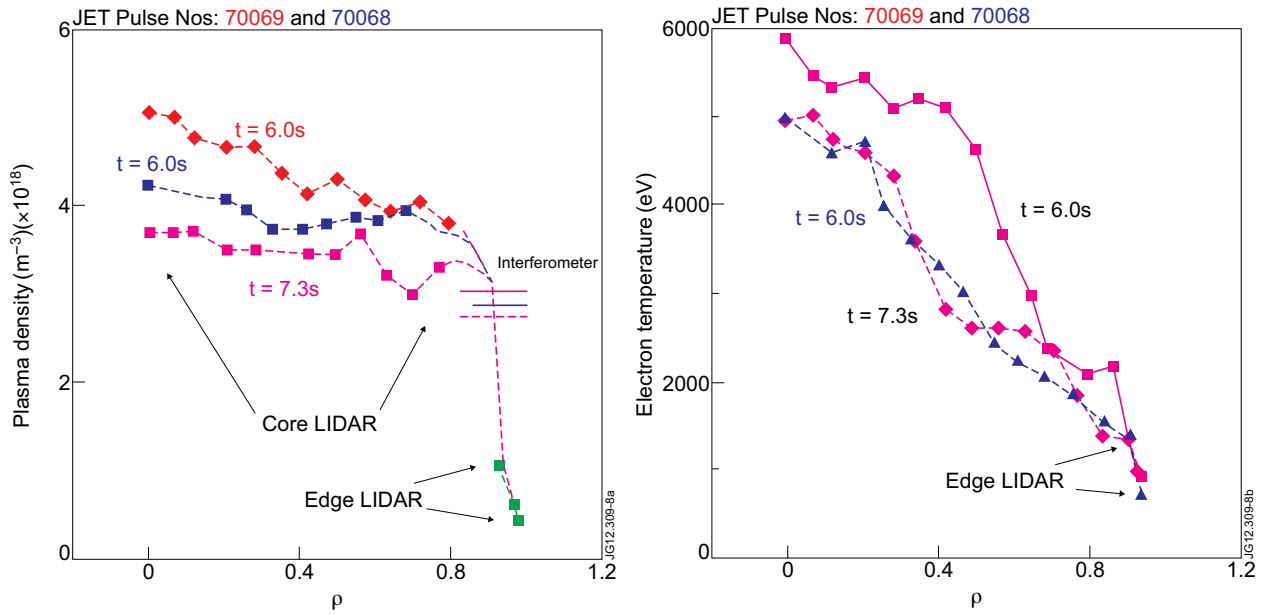


Figure 10: Electron plasma a) density and b) temperature profiles of experiments of Fig.10. Pulse No: 70069 having a high  $\beta_N$  phase: the profiles at  $t = 6.0s$  are obtained by averaging the available data from  $t = 5.5s$  and  $t = 6.5s$ , and they at  $t = 7.3s$  are obtained by average from  $t = 6.8s$  to  $t = 7.8s$ . Pulse No: 70068: the profiles at  $t = 6.0s$  are obtained by data averaged from  $t = 5.5s$  to  $t = 6.5s$ .

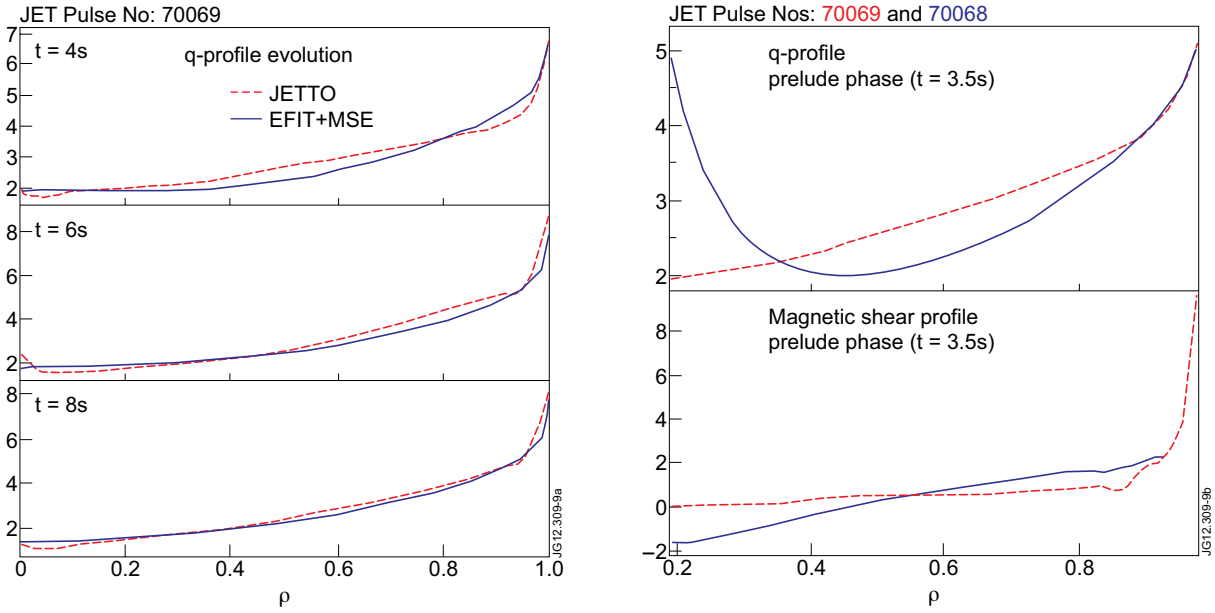


Figure 11: a):  $q$ -profile evolution during the main heating phase at three different time points as obtained by the modelling of JETTO and compared with the available EFIT+MSE data measurements for the Pulse No: 70069 of Fig 10. b):  $q$  and c)  $s$ -profile in the prelude phases (at  $t = 3.5s$ ) of the Pulse No: 70068 of Fig.10.

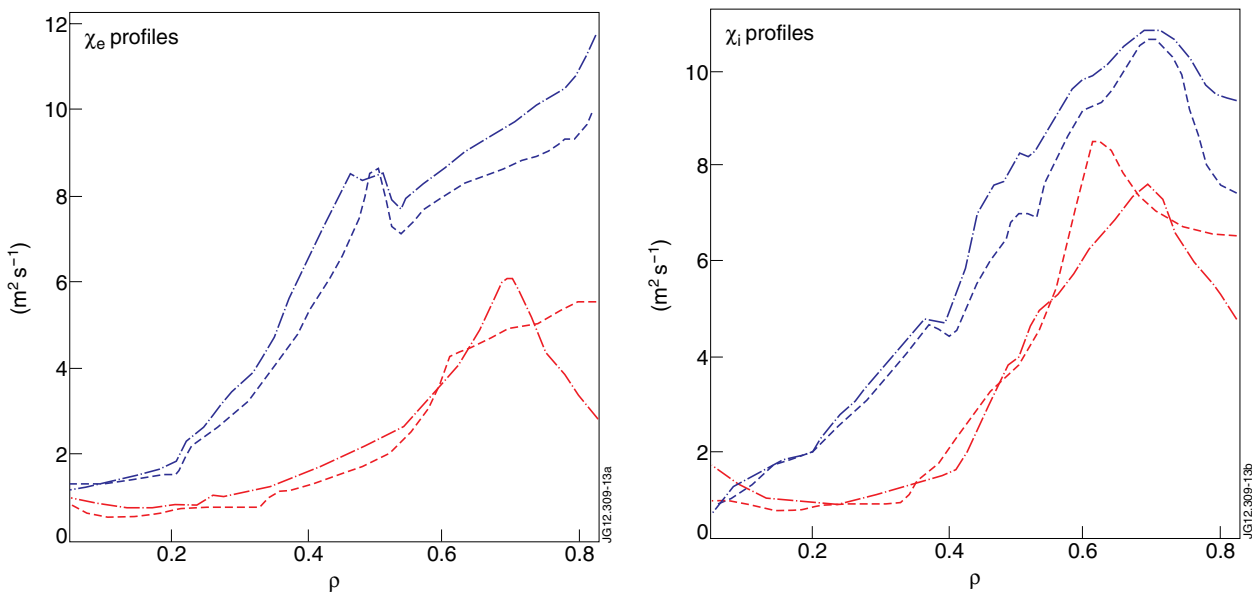


Figure 13: Thermal diffusivity at different time points of Pulse No: 70069 of Fig.10, during the high  $\beta_N$  phase (red curves: 5.5s dashes, 6.0s dot-dashes) and after its termination (blue curves: 7.3s dashes, 7.8s dot-dashes).

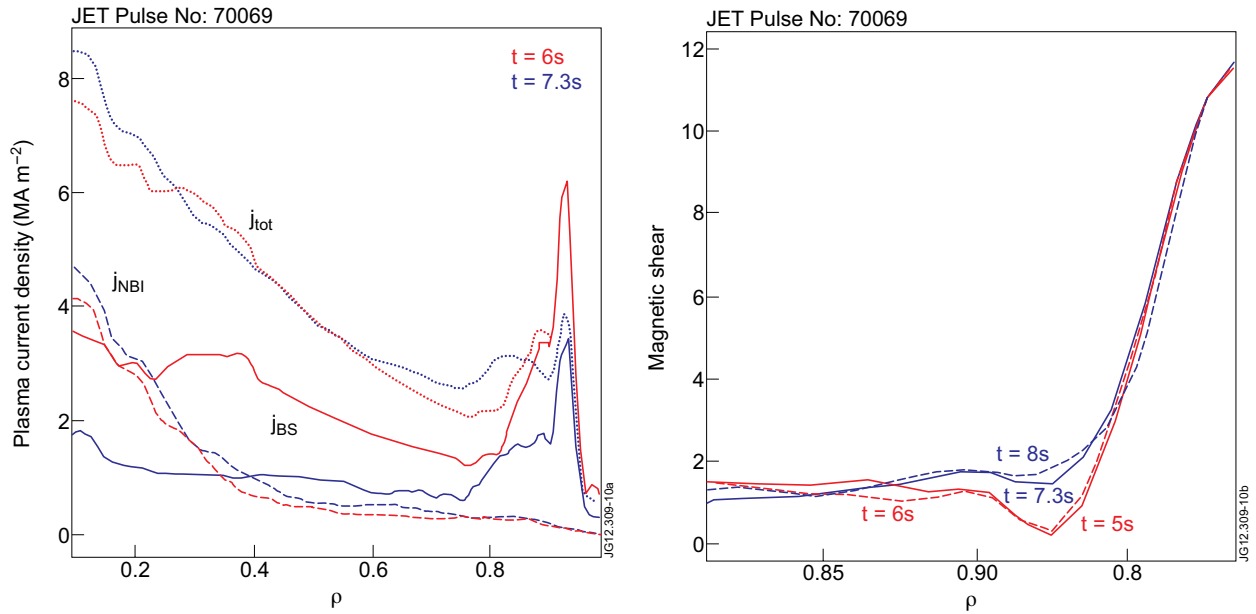


Figure 14: (a) Modelling of the plasma current density profile evolution, for Pulse No: 70069 of Fig.10. The contributions of NB and bootstrap current density are evidenced. Two time points are considered, as representative of the phases of high  $\beta_N$  (at  $t = 6.0\text{s}$ ) and after TB collapse ( $t = 7.3\text{s}$ ). (b) Evolution of the magnetic shear radial profile of Pulse No: 70069. The two different times points are representative of the main heating phase in presence of TB ( $t = 5.0\text{s} - 6.0\text{s}$ ) and after its collapse ( $t = 7.3\text{s} - 8.0\text{s}$ ). The available data averaged over  $\pm 0.5\text{s}$  at around the nominal time point have been considered.